February 16, 2001

Photoelectron Yield

Fall 2000 Test Run

G. Mitchell

During the test run, the photoelectron yield of the four CsI(Tl) detector channels was estimated by placing a boron carbide target in the neutron beam. Using the measured neutron flux at 4 meV and the size of the detector signals, and accounting for factors of beam attenuation and detector acceptance, the four detectors saw 1350, 1230, 570, and 320 photoelectrons per MeV of deposited energy. This performance is sufficient for NPDGamma.

Introduction

The NPDGamma experiment requires that a large number of photoelectrons be produced per MeV deposited in the detector crystals. This will minimize the contribution of shot noise to the experimental error and reduce the amount of time necessary to measure the noise contribution of the amplifier electronics. An acceptable number, given in the proposal [1], is 500 photoelectrons per 2.2 MeV gamma. In the Fall 2000 Test Run, 3 in. photodiodes were used to detect the light from the four CsI(Tl) detectors. The 3 in. photodiodes are clearly superior to the candidate 5 in. models in their insensitivity to magnetic fields [2], but due to their smaller size and thus lower light collection efficiency, their photoelectron yield needed to be verified as acceptable.

Method

The number of photoelectrons per MeV was measured during the test run [3] using a target that produced gammas of known energy following neutron capture. A 3/8 in. thick boron carbide (B_4C) target was placed in the area between the four detectors, indicated in Fig. 1. The density of boron carbide is 2.52 g/cm^3, the molecular weight is 55.26, and the natural ^{10}B isotopic fraction is 19.6%. Due to the large neutron cross-section for ^{10}B ($\sigma \approx 7$ kb at 4 meV), this target was sufficiently thick to stop the entire neutron beam at low energies.

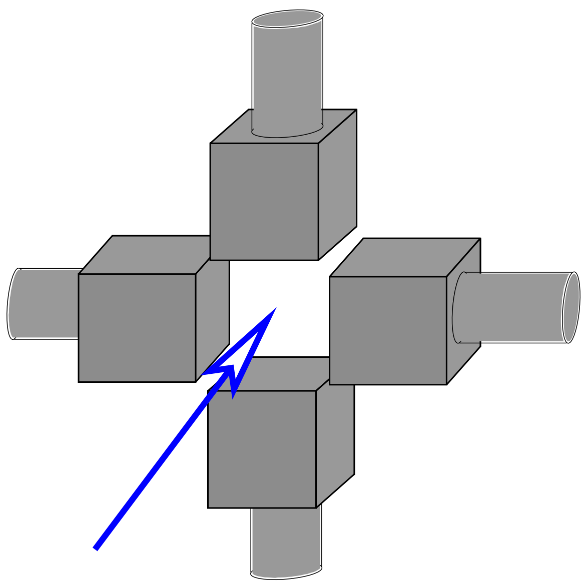

Figure 1: The four CsI(Tl) detectors with the photodiode housings. The crystals are $6 \times 6.5 \times 6.5$ in. The blue arrow indicates the direction of the neutron beam (into the page) and the tip of the arrow is the location of the boron carbide target.

The capture process for neutrons on ^{10}B proceeds via one of two channels [4]:

$$\mathrm{n} + {}^{10}\mathrm{B} \rightarrow \alpha + {}^{7}\mathrm{Li}\,(\mathrm{g.s.}) + 2.790\ \mathrm{MeV} \qquad (6.3\%)$$

$$\rightarrow \alpha + {}^{7}\mathrm{Li}^{*} + 2.312\ \mathrm{MeV} \qquad (93.7\%)$$

where the second channel is followed by $^{7}\mathrm{Li}^{*} \rightarrow {}^{7}\mathrm{Li(g.s.)} + \gamma$ with a gamma energy of 0.478 MeV. For determining the number of photoelectrons, these gammas were the useful result of the capture process. Due to the relatively large neutron cross-section for ^{10}B, all gammas are assumed to come from neutron capture on the ^{10}B. If the number of neutrons incident on the target is known, the gamma flux can be calculated.

Neutron Flux

The neutron flux out of the end of the guide was measured during the test run [5]. At 4 meV, the measured flux is reported as 8.66×10^5 neutrons/ms. This number should be adjusted for use here. The full-width at half maximum used to calculate this flux was based on a predicted energy dependence, and the prediction is systematically low. The measured FWHM at 4 meV was 4.55 cm, compared to the predicted FWHM of 4.15 cm. This leads to a correction factor of $(4.55/4.15)^2 = 1.2$. The calculation did not account for attenuation due to air. However, this attenuation will also be ignored here since the path length is identical. Since the flux measurement was performed at proton current of 90 μA, and this photoelectron measurement at 99 μA, an additional correction factor of 99 μA / 90 μA = 1.1 is necessary.

The beam was significantly attenuated due to the presence of the ^{3}He spin filter system, which was in place and polarized during this measurement with the boron carbide target. The ^{3}He system was not in place during the flux measurement. Following Ref. [6], the transmission T_n through the ^{3}He cell is calculated by

$$T_n = e^{-n_3\sigma\ell}\cosh(n_3\sigma\ell P_3)$$

where n_3 is the number density of ^{3}He, σ is the ^{3}He neutron cross-section, ℓ is the length of the cell, and P_3 is the polarization. When warm, the cell thickness was $n_3\ell = 6.0$ amagat $\cdot$ cm $= 1.61 \times 10^{20}/\text{cm}^2$, where 1 amagat $= 2.6868 \times 10^{19}/\text{cm}^3$. Assuming a $1/v$ dependence, at 4 meV the ^{3}He neutron cross-section is 13 kb. A typical value for the polarization was $P_3 = 26.5\%$. Combining these factors gives $n_3 \sigma \ell = 2.09$ and $n_3 \sigma \ell P_3 = 0.555$, resulting in $T_n = 0.143$.

A large sheet of 1 in. thick poly was located at z = 1.4 m downstream of the end of the neutron guide. The boron carbide target was located at z = 2.41 m. The poly sheet was used as a collimator and had a 2 in. diameter hole for the neutron beam. Based on the flux measurement, which included measurements of the beam width, the FWHM of the 4 meV neutron beam at z = 1.4 m was approximately 2.2 cm, which is half the diameter of the collimation. Therefore this collimation is neglected in calculating the neutron flux at the boron carbide target.

Combining the above factors affecting the neutron flux, the total flux incident on the boron carbide target at 4 meV was:

$$8.66 \times 10^5 \text{ neutrons/ms } \times 1.2 \times 1.1 \times 0.143 = 1.63 \times 10^8 \text{ neutrons/s.}$$

Detector Solid Angle

The gammas emitted following neutron capture by ^{10}B are assumed to be isotropic. The solid angle subtended by each detector is calculated as shown in Fig. 2. The crystal dimensions, taking c to be the distance from the center of the target area to the near face of the crystal, are $2a = 6$ in., $2b = 6.5$ in., and $c = 3.375$ in. The solid angle covered by the near detector face is $\Omega = 4\tan^{-1}(ab/d^2) = 1.22$ sr, so the fraction of 4π covered is 0.097. This is an overestimate of the effective solid angle, since gammas passing through the corners of the detector will not deposit all of their energy in the crystal. However, this overestimate leads to a lower result for photoelectrons per MeV, so it will be used regardless. Using $c = 8.875$ in., the distance to the far face of the crystal, gives $\Omega = 0.33$ sr, a factor of four difference.

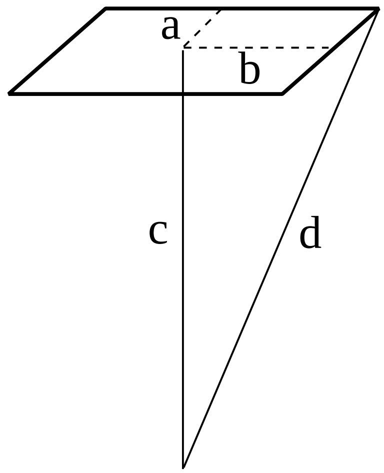

Figure 2: The solid angle subtended by a rectangle of dimension $2a$ by $2b$ at a distance c is $\Omega = 4\tan^{-1}(ab/d^2)$. The distance d to the corner of the rectangle is $d = \sqrt{a^2 + b^2 + c^2}$.

Results

With the boron carbide target in place, the channel 0 (upper) detector signal at 25 ms time of flight (corresponding to 4 meV neutrons) was measured to be 200 mV on an oscilloscope. As noted above, the proton current at this time was 99 μA. A typical pedestal value for channel 0 was 200 ADC counts ($\pm$ 50 counts), and at 0.3 mV per ADC count this means that the gamma signal in the detector was responsible for 140 mV of the signal. The gain resistor in the preamplifier circuit was 100 MΩ, so this is equivalent to a current of 0.14 V/$1{\times}10^8\,\Omega$= 1.4×10^{-9} A. Converting to photoelectrons, this is

$$(1.4 \times 10^{-9}\ \mathrm{C/s}) \times (1\ \mathrm{photoelectron}/1.602 \times 10^{-19}\ \mathrm{C}) = 8.7 \times 10^9\ \mathrm{photoelectrons/s}.$$

From above, the neutron flux on the boron carbide was 1.63×10^8 neutrons/s. Accounting for the probability to emit a gamma in ^{10}B neutron capture (factor of 0.937), the gamma energy (0.478 MeV), and the solid angle of the detector (factor of 0.097), the rate of energy deposit in the detector was

$$1.63 \times 10^8 \text{ neutrons/s } \times 0.937\ \gamma/\text{neutron } \times 0.478\ \text{MeV}/\gamma \times 0.097 = 7.08 \times 10^6\ \text{MeV/s}.$$

Therefore, the number of photoelectrons per MeV seen by detector channel 0 was

$$(8.7 \times 10^9 \text{ photoelectrons/s})/(7.08 \times 10^6 \text{ MeV/s}) = 1230 \text{ photoelectrons/MeV}.$$

Results for the other detectors are obtained from scaling by their gains, as determined from a run with the chlorine target. The photoelectrons yield of the four detectors is summarized in Table 1. The largest error in this calculation is due to the effective solid angle of the detectors, which could result in these calculations being up to a factor of two too low. Another possible error is the transmission of the ^{3}He. The transmission is dependent on the polarization, which was not recorded in the main log book for this measurement. The other parts of this photoelectron yield calculation are correct to 10%.

According to [7], the intrinsic light output of CsI(Tl) is 16000 photons per MeV. The number of photoelectrons seen in the test run is consistent with this number, given probable factors of light collection efficiency and quantum efficiency of the photodiodes.

channel	detector	typical signal	scale factor	photoelectrons/MeV
0	upper	10548	1.00	1230
1	right	4876	0.46	570
2	lower	2767	0.26	320
3	left	11653	1.10	1350

Table 1: Summary of photoelectron yield for the four detector channels in the Fall 2000 Test Run. The typical signal column is the average ADC counts registered in time bin 32 for each channel from run 3300, a run with the chlorine target in place. One ADC count $\approx$ 0.3 mV.

Conclusions

The photoelectron yields seen with the 3 in. photodiodes in the Fall 2000 Test Run, greater than 300 photoelectrons per MeV in each detector channel, were sufficiently large for NPDGamma. The figure assumed in the proposal is 225 photoelectrons per MeV. A more accurate estimation of the photoelectron yields would require a better estimate of the effective solid angle coverage of each detector.

The variation in the detector gains between the channels was disturbingly large, and the source of the variation needs to be understood. Bench testing of the CsI(Tl) crystals and photodiodes should identify which parts of the detector system are responsible for this variation.

References

[1] NPDGamma proposal: 'Measurement of the Parity-Violating Gamma Asymmetry A_γ in the Capture of Polarized Cold Neutrons by Para-Hydrogen, $\vec{n}+p \to d+\gamma$,' Bowman, J. D., *et al.*, 4/17/1998. Relevant pages: 38-40, 60-62, 67-70.

[2] Mitchell, G., 'Magnetic Field Effects on NPDGamma Photodiodes,' NPDGamma Technical Note, August 2000.

[3] NPDGamma Main Logbook I, pp. 262-263, 266, 9/23/2000.

[4] Yen, Y.-F., *et al.*, 'A high-rate ^{10}B-loaded liquid scintillation detector for parity-violation studies in neutron resonances,' Nucl. Instrum. Meth. **A447**, 476 (2000).

[5] Mitchell, G., 'Absolute Flux Measurement,' NPDGamma Technical Note, December 2000.

[6] Smith, T., 'NPDGamma Polarized ^{3}He Spin Filter Technical Note,' November 2000.

[7] Particle Data Group, 'Review of Particle Properties,' Phys. Rev. **D50**, 1173 (1994). Relevant section: Particle Detectors, p. 1261.